Polyhedron 29 (2010) 2667–2673

Contents lists available at ScienceDirect

Polyhedron

journal homepage: www.elsevier.com/locate/poly

Syntheses, structure characterisation and X-ray structures of the complexes $Ru_3(CO)_{11}L$ [L = $Ph_2P(C_6H_4Me$-*p*), $Ph_2PC_6F_5$, $P(C_6H_4Cl$-*p*$)_3$, $P(3,5$-CF_3–$C_6H_3)_3$ and $P(C_6H_4Me$-*p*$)_3$]

Omar bin Shawkataly [a,*], Mohd. Aslam A. Pankhi [a], Hoong-Kun Fun [b], Chin Sing Yeap [b]

[a] *Chemical Sciences Programme, School of Distance Education, Universiti Sains Malaysia, 11800 USM, Penang, Malaysia*
[b] *X-ray Crystallography Unit, School of Physics, Universiti Sains Malaysia, 11800 USM, Penang, Malaysia*

A R T I C L E I N F O

Article history:
Received 9 March 2010
Accepted 11 June 2010
Available online 30 June 2010

Keywords:
Ruthenium
Cluster
Carbonyl
Phosphines
X-ray diffraction

A B S T R A C T

Five trinuclear monosubstituted complexes of the type $Ru_3(CO)_{11}L$ were synthesised by the reaction of $Ru_3(CO)_{12}$ with phosphine ligands (L) using the radical anion catalysed method. The structures of the resulting clusters were elucidated by means of elemental analyses and spectroscopic methods, including IR, ^1H NMR, ^{13}C NMR and ^{31}P NMR spectroscopy. ^{31}P NMR spectra of the complexes $Ru_3(CO)_{11}P(C_6H_4Me$-*p*$)_3$ and $Ru_3(CO)_{11}P(C_6H_4Cl$-*p*$)_3$ showed splitting of the phosphorus signals into triplets. X-ray crystallographic studies of all five complexes were carried out. Out of the three unidentate tertiary phosphine complexes, $Ru_3(CO)_{11}P(C_6H_4Me$-*p*$)_3$ and $Ru_3(CO)_{11}P(C_6H_4Cl$-*p*$)_3$ are ordered while the complex $Ru_3(CO)_{11}P(3,5$-CF_3–$C_6H_3)_3$ exhibits disorder with respect to the trifluoromethyl groups.

In all the five monosubstituted complexes, the ligand occupies the equatorial position due to steric reasons and coordination of the ligands are only at the phosphorus atom. The effect of substitution resulted in significant differences in the Ru–Ru distances. Out of the three Ru–Ru bonds, the one which is *cis* to the ligand is noticeably longer and the mean value for this longest Ru–Ru bond is 2.889 Å, while the mean value for the two shorter Ru–Ru bonds is 2.841 Å. The P–C distances are in the range 2.333(6)–2.354(6) Å. The equatorial Ru–CO moieties are almost linear and the average value for all the five complexes studied range from 176.3 to 177.6°, while the axial CO groups are slightly bent, ranging from 173.8 to 174.1°.

1. Introduction

The syntheses and crystallographic structures of substituted triangular triruthenium clusters have been of interest to researchers due to their structural variation and catalytic activity [1]. It is known that the usual product of the reaction between $Ru_3(CO)_{12}$ and tertiary phosphines, PR_3, is the tri-substituted complex $Ru_3(CO)_9(PR_3)_3$; mono- and di-substituted complexes have been obtained earlier only under special conditions, such as under CO, or as by-products from reactions designed to afford other products. An earlier method reported by Bruce et al. was the displacement method whereby the complex $Ru_3(CO)_{11}(CNBu^t)$ was made to react with CO or a ligand containing P, As or Sb as the donor element, by displacing CO or $CNBu^t$ [2]. This method resulted in products with poor yields as by-products are also formed, though the usefulness of this process has been successfully demonstrated for synthesising monosubstituted complexes of $Os_3(CO)_{12}$ by the reaction of $Os_3(CO)_{11}(CH_3CN)$ with PR_3 [3,4]. Other methods to synthesise this type of complex are the amine oxide/MeCN method [5] and also salts of the bis(triphenylphosphine) iminium ion, PPN^+ [6]. However, we prefer the radical anion method, as developed by Bruce et al., to synthesise derivatives of the type $Ru_3(CO)_{12-n}L_n$ [n = 1–4], substituted by tertiary phosphines, phosphites, arsines and isocyanides [7,8a,b]. Substitution of CO by a more bulky ligand results in the latter ligand occupying the sterically least demanding site, which in all the cases is the equatorial site.

Many monosubstituted complexes have been synthesised in the past using the radical anion method, but few have been crystallographically studied. Specially, for complexes of $Ru_3(CO)_{12}$ with ligands of the type Ph_2PR (monosubstituted diphenylphosphine), only three complexes have been crystallographically characterised [9–11]. Phosphine ligands have found extensive use in the formation of many complexes of ruthenium over the years. Recently the reaction of $Ru_3(CO)_{12}$ with tris(2-furyl) phosphine has been investigated [12a]. The same author also mentions the reaction of $Ru_3(CO)_{12}$ with tris(2-thienyl) phosphine via electron transfer catalysis conditions, which resulted in mono-, di- and tri-substituted derivatives [12b].

---

* Corresponding author. Address: Multimedia University, Melaka Campus, Jalan Ayer Keroh Lama, 74750 Melaka, Malaysia. Tel.: +60 4 653 3936; fax: +60 4 657 6000.
E-mail address: omarsa@usm.my (O.b. Shawkataly).

0277-5387/$ - see front matter © 2010 Elsevier Ltd. All rights reserved.
doi:10.1016/j.poly.2010.06.013

Besides the monosubstituted complexes reported in this paper, di- and tri-substituted complexes (of the type $Ru_3(CO)_{10}L_2$ and $Ru_3(CO)_9L_3$, respectively) have also been synthesised by us and their structures crystallographically studied, which will be communicated later [13]. To further our interest on substituted triangle triruthenium clusters, we report the syntheses, characterisation of $Ru_3(CO)_{11}L$ [L = $Ph_2P(C_6H_4Me$-*p*) **1a**, $Ph_2PC_6F_5$ **1b**, P(C_6H_4Cl-*p*)$_3$ **1c**, P(3,5-CF_3–C_6H_3)$_3$ **1d**, P(C_6H_4Me-*p*)$_3$ **1e**, PhP($C_6H_4OCH_3$-*p*)$_2$ **1f**]. However whilst X-ray studies of five complexes, **1a**–**e**, have been carried out, **1f** was excluded as it was not possible to obtain single crystals suitable for XRD studies. The synthesis of **1e** has been reported earlier [2], but X-ray diffraction studies have been carried out in this paper along with spectral studies, especially ^{31}P NMR.

The effect of substitution on the triruthenium cluster manifests itself in many ways, with the decrease in the molecular symmetry. Introduction of a non-CO ligand, in general, to $Ru_3(CO)_{12}$ results in a lengthening of the Ru–Ru bond. A trend has been reasonably well observed in all the substituted complexes (**1a**–**e**). In the light of other published reports on monosubstituted clusters of $Ru_3(CO)_{12}$, this study enabled us to make a more extensive comparison on the changes in the molecular geometries resulting from substitution of CO by different ligands. The monosubstituted clusters, which have been synthesised in good yield, will also make interesting precursors for a range of mixed-ligand complexes and other disubstituted complexes.

2. Experimental

2.1. Chemicals, starting materials and spectroscopic measurements

All the syntheses were carried out using standard Schlenk techniques under an atmosphere of nitrogen. $Ru_3(CO)_{12}$ (Aldrich), $Ph_2P(C_6H_4Me$-*p*) (Pressure Chemical Co., USA), $Ph_2PC_6F_5$, P(3,5-CF_3–C_6H_3)$_3$, P(C_6H_4Cl-*p*)$_3$, P(C_6H_4Me-*p*)$_3$ and PhP($C_6H_4OCH_3$-*p*)$_2$ (Maybridge Chemical Co., Ltd., UK) were used as received. Tetrahydrofuran was distilled from sodium benzophenone ketyl under a dry oxygen-free nitrogen atmosphere. The radical anion method was used for the syntheses of the complexes [14]. AR grade solvents were used for crystallisation. Florisil (100–200 mesh, Acros) was used as the stationary phase for column chromatography. Preparative TLC was carried out on glass plates 20 × 20 cm using Silica gel $60GF_{254}$ (Merck). Hexane and dichloromethane of AR grades were used for elution during the column chromatography and preparative TLC. Elemental analyses were performed using a Perkin–Elmer model 2400 LS Series II C, H, N analyser equipment, USA. The melting points of the compounds were recorded in open capillaries using an SMP1 melting point apparatus, UK and were uncorrected. IR spectra were recorded with a Perkin–Elmer System 2000 FTIR spectrometer in a NaCl solution cell (0.1 mm). Deuterated chloroform was used as a solvent for ^{1}H NMR, ^{13}C NMR and ^{31}P NMR spectra. These NMR studies were carried out on Bruker B2H 400 FT-NMR spectrometer using 5 mm tubes. The ^{1}H NMR and ^{13}C NMR shifts were referenced to TMS and ^{31}P NMR shifts were referenced to 85% H_3PO_4.

Compounds **1a–e** were prepared in high yield by an electron transfer catalysed reaction between $Ru_3(CO)_{12}$ and a stoichiometric amount of the appropriate ligand. The resulting complexes were separated by means of column chromatography and then isolated in the pure form. Complexes **1a–f** were characterised by elemental microanalyses and their spectral studies.

2.2. Synthesis of the metal complexes

2.2.1. General procedure for the synthesis of complexes 1b–f

$Ru_3(CO)_{12}$ and the appropriate phosphine ligand (in the ratio 1:1.05) in 10 ml dry deoxygenated THF were heated in an oil bath and warmed to 40 °C to dissolve the $Ru_3(CO)_{12}$. Sodium benzophenone ketyl solution (five drops) was added via syringe, which was followed immediately by a darkening of the reaction solution (red). After TLC showed completion of the reaction, the solvent was removed under reduced pressure to give a red residue. Thin layer chromatography showed the presence of two spots, one of them being the starting material $Ru_3(CO)_{12}$ in traces. This was identified by its IR *v* (CO) spectrum with that of an authentic sample. The major orange band was separated by column chromatography and characterised.

2.2.2. Synthesis of undecacarbonyl (p-tolyldiphenylphosphino) triruthenium 1a

$Ru_3(CO)_{12}$ (100.0 mg, 0.156 mmol) and $Ph_2P(C_6H_4Me$-*p*) (45.4 mg, 0.164 mmol) in 10 ml dry deoxygenated THF were heated in an oil bath and warmed to 40 °C to dissolve the $Ru_3(CO)_{12}$. Sodium benzophenone ketyl solution (five drops) was added dropwise via a syringe, which immediately changed the reaction solution to red. After TLC showed completion of the reaction, the solvent was removed under reduced pressure to give an oily mass. Thin layer chromatography showed the presence of three spots including traces of the starting material $Ru_3(CO)_{12}$, identified by its TLC and IR *v* (CO) spectrum with that of an authentic sample. The major orange band was separated by column chromatography (dichloromethane and hexane) and characterised. Yield: 88.8 mg (64%), m.p. 148–150 °C.

Elemental *Anal.* Calc. for $Ru_3C_{30}H_{17}O_{11}P$: C, 40.59; H, 1.25. Found: C, 40.57; H, 1.26%. IR (cyclohexane), *v* (CO) 2097m, 2058w, 2045s, 2015vs, 1988m cm^{-1}. ^{1}H NMR ($CDCl_3$) δ 2.40 (s, 3H, CH_3), 7.23–7.50 (m, 14H, Ph). ^{13}C NMR ($CDCl_3$) δ 21.6 (CH_3), 128.9–135.9 (m, Ph), 204.6 (m, CO). ^{31}P NMR ($CDCl_3$) δ 35.50–35.54 (d, $Ph_2PC_6H_4Me$-*p*). Crystals suitable for X-ray crystallography were grown by slow evaporation of a *n*-hexane solution at 10 °C.

A third band (red), which was more polar than the major orange band, could not be separated by column chromatography. However, thin layer chromatography showed the compound to be $Ru_3(CO)_{10}$-($Ph_2PC_6H_4Me$-*p*)$_2$. Another complex was synthesised by the reaction of $Ru_3(CO)_{12}$ and $Ph_2P(C_6H_4Me$-*p*) in a 1:2 molar ratio in THF at 40 °C. Preparative TLC showed two bands including a small amount of $Ru_3(CO)_{11}Ph_2P(C_6H_4Me$-*p*) [$R_f$ = 0.54], identified by its IR and TLC with **1a**. The major red band was separated; hexane:dichloromethane; 80:20; R_f = 0.40. IR (cyclohexane) showed the absence of a band at 2097 cm^{-1}, but exhibited a band at 2075 cm^{-1}, indicative of the disubstituted $Ru_3(CO)_{10}[Ph_2P(C_6H_4Me$-*p*)]$_2$. Attempts to grow suitable single crystals of this compound for XRD studies were not successful. Yield: 72.0 mg (50%). Elemental *Anal.* Calc. for $Ru_3C_{48}H_{34}O_{10}P_2$: C, 50.75; H, 3.02. Found: C, 50.70; H, 3.05%. IR (cyclohexane), *v* (CO) 2075m, 2059s, 2042m, 2019s, 1990s cm^{-1}. ^{1}H NMR ($CDCl_3$) δ 2.40 (s, 6H, CH_3), 7.22–7.51 (m, 28H, Ph). ^{13}C NMR ($CDCl_3$) δ 21.4 (–CH_3), 129.0–137.4 (m, Ph), 141.9 (C–CH_3), 204.6 (m, CO).

2.2.3. Undecacarbonyl (diphenyl pentafluorophenyl phosphino) triruthenium 1b

Yield: 93.4 mg (62%), m.p. 127–129 °C. Elemental *Anal.* Calc. for $Ru_3C_{29}H_{10}O_{11}F_5P$: C, 36.14; H, 1.04. Found: C, 36.11; H, 1.06%. IR (cyclohexane), *v* (CO) 2101m, 2050m, 2030m, 2019s, 1989m cm^{-1}. ^{1}H NMR ($CDCl_3$) δ 7.35–7.70 (m, 10H, Ph). ^{13}C NMR ($CDCl_3$) δ 128.2–132.2 (m, Ph), 202.8 (m, CO). ^{31}P NMR ($CDCl_3$) δ 28.6 (s, $Ph_2PC_6F_5$). Crystals suitable for X-ray crystallography were grown by slow evaporation of a *n*-hexane solution at 10 °C.

2.2.4. Undecacarbonyl (tris-p-chlorophenylphosphino) triruthenium 1c

Yield: 99.3 mg (65%), m.p. 156–158 °C. Elemental *Anal.* Calc. for $Ru_3C_{29}H_{12}O_{11}Cl_3P$: C, 35.65; H, 1.23. Found: C, 35.61; H, 1.22%. IR (cyclohexane), ν (CO) 2099m, 2060w, 2048m, 2032sh, 2018s, 1989m cm^{-1}. ^{1}H NMR (CDCl$_3$) δ 7.35–7.49 (m, 12H, Ph). ^{13}C NMR (CDCl$_3$) δ 129.1–133.2 (m, Ph), 203.6 (m, CO). ^{31}P NMR (CDCl$_3$) δ 35.1–35.3 [t, P(C$_6$H$_4$-Cl-*p*)$_3$]. Crystals suitable for X-ray crystallography were grown from a solution of *n*-hexane/dichloromethane at 10 °C.

2.2.5. Undecacarbonyl [tris(bis3,5-trifluoromethyl)phosphino] triruthenium **1d**

Yield: 128 mg (64%), m.p. 132–134 °C. Elemental *Anal.* Calc. for Ru$_3$C$_{35}$H$_9$O$_{11}$F$_{18}$P: C, 32.80; H, 0.70. Found: C, 32.81; H, 0.71%. IR (cyclohexane), ν (CO) 2106m, 2057s, 2038m, 2026s, 2006sh, 1991s cm^{-1}. ^{1}H NMR (CDCl$_3$) δ 7.30–8.16 (m, 9H, Ph). ^{13}C NMR (CDCl$_3$) δ 120.96–137.4 (m, Ph and tetrahedral carbons), 202.8 (m, CO). ^{31}P NMR (CDCl$_3$) δ 41.56 (s, P ligand). Crystals suitable for X-ray crystallography were grown by slow evaporation of a *n*-pentane solution at 10 °C.

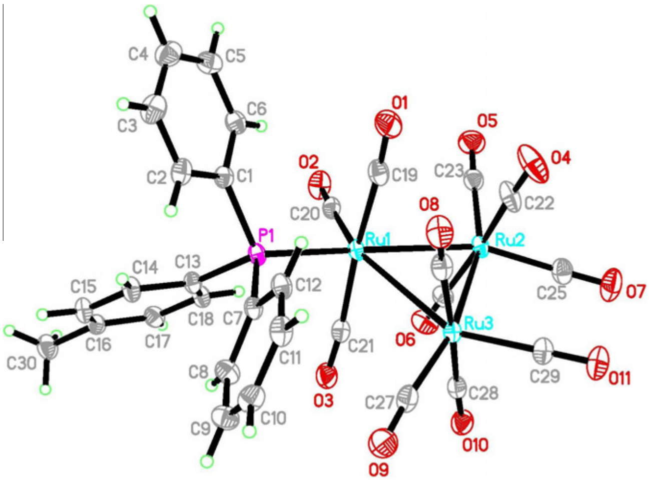

Fig. 1. The ORTEP diagram of **1a** with 50% probability ellipsoids for non-H atoms.

2.2.6. Undecacarbonyl (tris-4-methylphenylphosphino) triruthenium **1e**

Yield: 98.8 mg (69%), m.p. 176–179 °C. Elemental *Anal.* Calc. for Ru$_3$C$_{32}$H$_{21}$O$_{11}$P: C, 41.97; H, 2.30. Found: C, 41.94; H, 2.29%. IR (cyclohexane), ν (CO) 2096m, 2059sh, 2044m, 2014s, 1989m cm^{-1}. ^{1}H NMR (CDCl$_3$) δ 2.35–2.45 (s, 9H, CH$_3$), 7.19–7.40 (m, Ph). ^{31}P NMR (CDCl$_3$) δ 34.4–34.6 [t, P(C$_6$H$_4$Me-*p*)$_3$]. X-ray quality crystals were grown from a *n*-hexane solution at 10 °C.

2.2.7. Reaction of Ru$_3$(CO)$_{12}$ with bis(4-methoxyphenyl) phenyl phosphine **1f**

Yield: 86 mg (58.9%). IR (cyclohexane), ν (CO) 2096m, 2059w, 2044m, 2014s, 1989s cm^{-1}. ^{1}H NMR (CDCl$_3$) δ 3.9 (s, 6H, OCH$_3$,), 6.9–7.5 (m, 13H, Ph). ^{13}C NMR (CDCl$_3$) δ 55.7 (–OCH$_3$), 125–136 (m, Ph), 161.6 (*C*–OCH$_3$), 204.6 (m, CO). All attempts to crystallise this compound to obtain single crystals suitable for XRD studies were not successful.

2.3. X-ray structural determination

Determination of cell constants and data collection were carried out at 100.0(1) K using the Oxford Cryosystem Cobra low-temperature attachment with Mo Kα radiation (λ = 0.71073) on a Bruker SMART APEX2 CCD area-detector diffractometer equipped with a graphite monochromator [15]. The data were reduced using SAINT [15]. A semi-empirical absorption correction was applied to the data using SADABS [15]. The structures were solved by direct methods and refined against F^2 by full-matrix least-squares using SHELXTL [16]. Hydrogen atoms were placed in calculated positions.

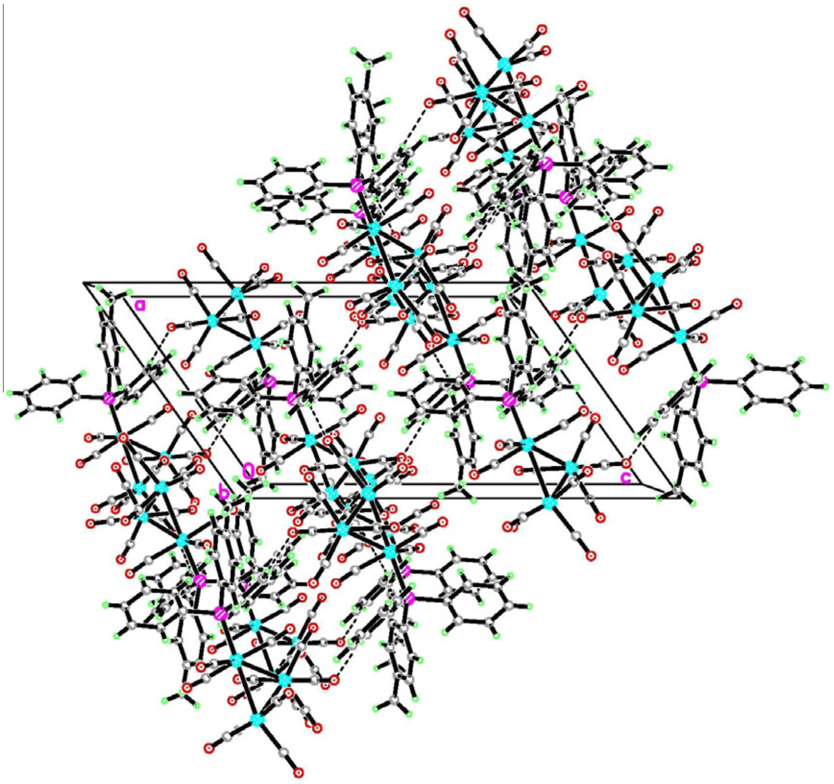

Fig. 2. The crystal packing of **1a**, viewed along the *b* axis, showing the molecules being linked into a 3-D network. Intermolecular hydrogen bonds are shown as dashed lines.

The ORTEP plot of $Ru_3(CO)_{11}(Ph_2PC_6H_4Me\text{-}p)$ is shown in Fig. 1. The dihedral angles between the methylphenyl ring and the two benzene rings for complex **1a** are 79.69(17)° and 61.21(18)°, respectively. Weak intermolecular C8–H8A···O10 = 3.259(4) Å and C11–H11A···O7 = 3.320(5) Å hydrogen bonds linked the complex **1a** molecules into a three-dimensional network (Fig. 2). For complex **1b**, the pentafluorophenyl ring makes dihedral angles of 71.46(19)° and 57.0(2)° with the other two benzene rings (The ORTEP plot of complex **1b** is shown in Fig. 3). The dihedral angles between the three phosphine-substituted rings are 63.68(7)°, 69.88(7)° and 78.74(7)° for complex **1c** (The ORTEP plot of **1c** is shown in Fig. 4). In complex **1d**; atoms F10, F11 and F12 are disordered over three positions with site occupancies fixed to 0.34, 0.33 and 0.33, respectively at the final refinement (The ORTEP plot of **1d** is shown in Fig. 5). The same U^{ij} parameters were used for the atom pairs F10A/F11A/F8/F12A and F12B/F11C. Complex **1d** is linked into a dimer by the intermolecular hydrogen bond C4–H4A···O5 = 3.452(3) Å (Fig. 6). The dihedral angles between the three phosphine-substituted rings are 50.38(11)°, 60.89(11)° and 83.02(11)° for complex **1d**. The ORTEP plot of $Ru_3(CO)_{11}P(C_6H_4\text{-}Me\text{-}p)_3$ is shown in Fig. 7. The dihedral angles between the three phosphine-substituted rings are 68.59(11)°, 60.64(11)° and 79.60(12)° for complex **1e**. Crystal data and experimental details of the structure determinations are listed in Table 1. Details of all hydrogen bonding geometry are listed in Table 3.

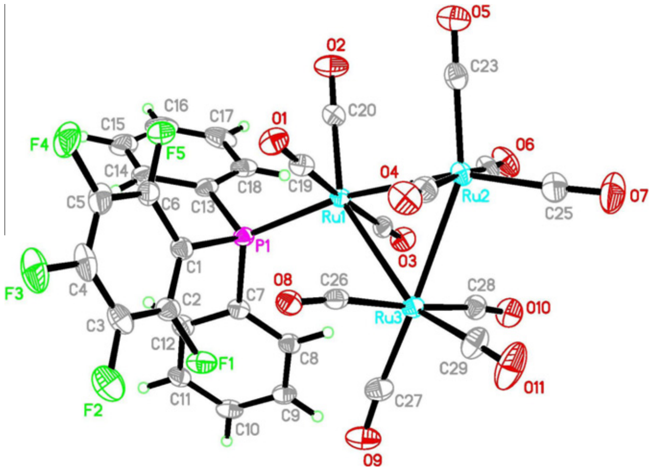

Fig. 3. The ORTEP diagram of **1b** with 50% probability ellipsoids for non-H atoms.

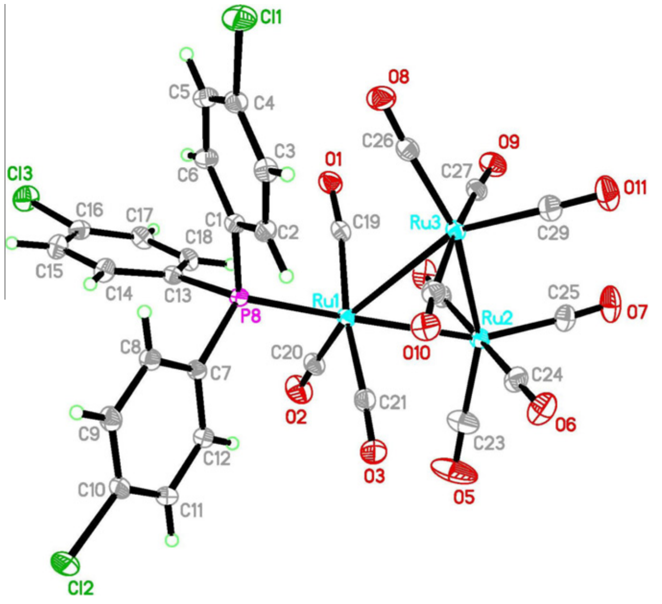

Fig. 4. The ORTEP diagram of **1c** with 50% probability ellipsoids for non-H atoms.

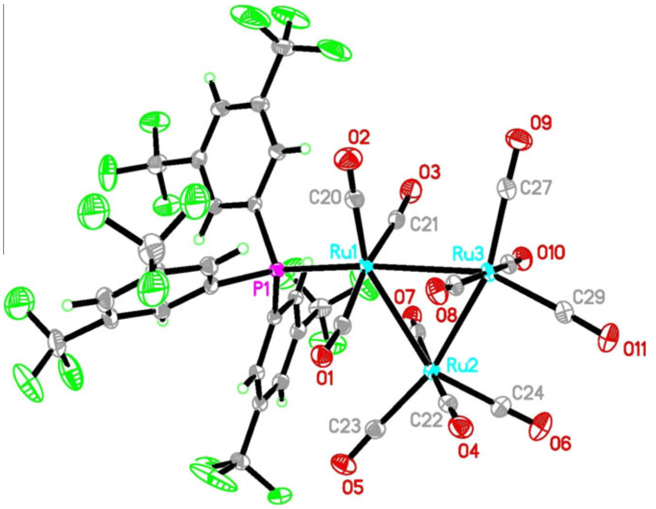

Fig. 5. The ORTEP diagram of **1d** with 50% probability ellipsoids for non-H atoms. Only the major disorder component is shown.

2.4. General structural considerations

The molecular structures of the five complexes **1a–e** have been determined. Table 2 summarises important bond lengths that are found for these complexes. A comparison has been made in the same table with $Ru_3(CO)_{12}$ and other monosubstituted complexes of the same type (references have been mentioned).

3. Results and discussion

3.1. Synthesis and characterisation

The microanalyses of all the compounds agreed well with the proposed molecular formulae for all the reported compounds within the experimental errors. Isolation of a number of substituted derivatives of $Ru_3(CO)_{12}$ has enabled definitive information on ν (CO) frequencies and the degree of substitution, which can be readily determined from IR spectra. It has been observed that monosubstituted clusters of $Ru_3(CO)_{12}$ are characterised by a high energy absorption around 2100 cm^{-1}. Similar observations were reported by Bruce et al. [8a]. Individual bands, however, may vary slightly in position and relative intensity. ^1H NMR spectra of **1a**–**c** and **e** showed a multiplet around δ 7.2–7.6 ppm, characteristic of phenyl groups. For the methyl groups, a singlet was observed at δ 2.4 for the $Ph_2P(C_6H_4Me\text{-}p)$ substituted cluster, and at δ 2.4 for the $P(C_6H_4Me\text{-}p)_3$ substituted cluster. In the case of **1d**, aromatic protons were downfield and observed at higher δ values due to $-CF_3$ groups (7.3–8.1 ppm). ^{13}C NMR spectra of all the substituted clusters showed prominent signals at around δ 125–137 ppm, characteristic of phenyl carbons. The carbonyl carbons in all the clusters exhibited a multiplet, as a single broad peak. The broadness of the single peak in the ^{13}C NMR suggests that the carbonyl ligands of the triruthenium cluster are fluxional in solution. A similar observation was made by Lam et al. when they investigated the reactions of 2-indolylphosphines with $Ru_3(CO)_{12}$ [11]. In addition, the methyl carbons appeared at δ 21 ppm for the cluster **1a**. In the case of the complex **1f**, the methoxy carbons appeared at δ 55 ppm, while the two tetrahedral carbons which are attached to

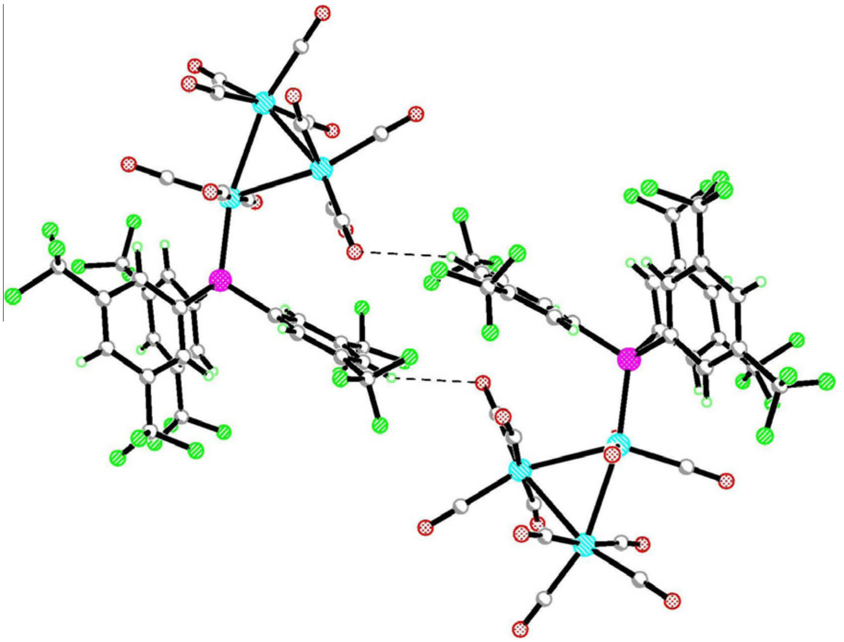

Fig. 6. The intermolecular hydrogen bond linking **1d** molecules into a dimer.

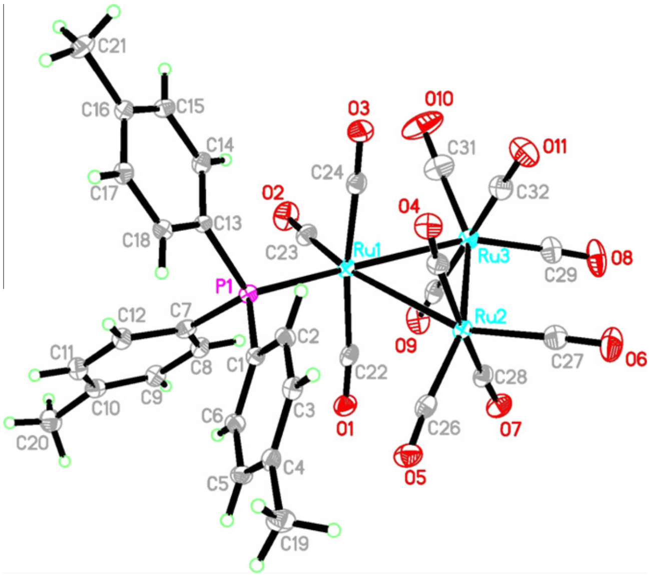

Fig. 7. The ORTEP diagram of **1e** with 50% probability ellipsoids for non-H atoms.

–OCH_3 groups were observed at δ 166 ppm. ^{31}P NMR spectra showed single signals at δ 28.5 and 41.5 ppm for complexes **1b** and **d,** respectively. For the $Ph_2P(C_6H_4Me\text{-}p)$ substituted cluster, a doublet appeared at δ 35.5 ppm, while in case of clusters containing a ligand of the type PR_3 (substituted at the para position), a triplet is observed. Thus, in the case of the complex substituted by the ligand $P(C_6H_4Cl\text{-}p)_3$, a triplet with J(PP) = 10.4 Hz is observed while a triplet with J(PP) = 11 Hz appeared in the case of the $P(C_6H_4Me\text{-}p)_3$ substituted cluster.

3.2. X-ray crystal structure analysis

The crystal structures of the five complexes **1a**–**e** have been determined. Table 2 summarises important bond lengths found for these complexes. All the compounds contain a triangular arrangement of three ruthenium atoms. The coordination of the ligand was observed only at the phosphorus atom and in each case the ligand occupies an equatorial site. In $Ru_3(CO)_{12}$, the average Ru–Ru separations are 2.854 Å [17], one of the three Ru–Ru bonds being slightly longer than the other two Ru–Ru bonds. The longest Ru–Ru bond in $Ru_3(CO)_{12}$ is 2.859 Å. In the five complexes studied (**1a**–**e**), the longest Ru–Ru bond is the bond that is *cis* to the ligand. For the complex containing the ligand $Ph_2PC_6F_5$, the longest Ru–Ru bond is 2.886(4) Å. For complexes **1c**–**e**, the longest Ru–Ru separations are 2.889(14), 2.888(2) and 2.884(2) Å, respectively. Among all the complexes (**1a**–**e**), the longest Ru–Ru bond has been observed for the complex $Ru_3(CO)_{11}(Ph_2PC_6H_4CH_3\text{-}p)$ (**1a**), and this is 2.896(3) Å. The uneven increase in the lengths of the metal–metal bonds in comparison with those in $Ru_3(CO)_{12}$ can be attributed to the steric effect induced by the bulky substituent. Another study carried out on $Os_3(CO)_{11}(PR_3)$ compounds establishes that the electronic effect of the P ligand could also contribute to the changes in the M–M bond lengths [18]. We have observed that Ru–Ru separations in all the complexes studied have ranges from 2.819(2) (for **1d**) to 2.896(3) Å (for **1a**). In the monosubstituted complexes of a similar type synthesised by Bruce et al., the Ru–Ru separations were reported to be in the range 2.839–2.920 Å [8a].

There are no significant differences in the Ru–P distances of all the complexes, the lowest being 2.333(6) Å for complex **1d** and the highest being 2.355(6) Å for complex **1e**. In all the complexes studied, the average Ru–P bond length is slightly shorter compared to the Ru–P bond length of 2.380(6) Å observed for $Ru_3(CO)_{11}(PPh_3)$, in which the P atom is similarly bonded equatorially to the ruthenium cluster [19]. Bruce et al. reported the range 2.238(1)–2.399(4) Å for the four complexes they studied. In their study, they correlated the shortest Ru–P bond length to the ligand with the smaller cone angle [8a]. In the complexes, the ligand is approximately *trans* to one of the Ru–Ru bonds, and the Ru–Ru–P angles among all the complexes range between 107.6(3)° for $Ru_3(CO)_{11}PPh_2C_6F_5$ and 113.0(9)° for $Ru_3(CO)_{11}P(C_6H_4Cl\text{-}p)_3$.

As observed in $Ru_3(CO)_{12}$, the bonds from the metal atom to the axial CO ligands are longer compared to the equatorial CO groups. In $Ru_3(CO)_{12}$, the axial Ru–CO distances range in length from 1.929(4) to 1.953(5) Å [average 1.942(4) Å], and the equatorial

Table 1
Crystal data and structure refinement parameters for **1a–e**.

Compound	**1a**	**1b**	**1c**	**1d**	**1e**
Empirical formula	$C_{30}H_{17}O_{11}PRu_3$	$C_{29}H_{10}F_5O_{11}PRu_3$	$C_{29}H_{12}Cl_3O_{11}PRu_3$	$C_{35}H_9F_{18}O_{11}PRu_3$	$C_{32}H_{21}O_{11}PRu_3$
Formula weight	887.62	963.55	976.92	1281.60	915.67
T (K)	100.0(1)	100.0(1)	100.0(1)	100.0(1)	100.0(1)
Wavelength (Å)	0.71073	0.71073	0.71073	0.71073	0.71073
Crystal system	monoclinic	monoclinic	triclinic	triclinic	triclinic
Space group	$P2_1/c$	$C2/c$	$P\bar{1}$	$P\bar{1}$	$P\bar{1}$
Unit cell dimensions					
a (Å)	12.0739(1)	42.2707(8)	9.5029(1)	12.0228(1)	9.6203(1)
b (Å)	15.4256(2)	9.0628(2)	12.4248(1)	12.5224(1)	12.3659(2)
c (Å)	20.2404(2)	16.3392(3)	15.0083(2)	14.4396(2)	15.3136(2)
α (°)	90	90	95.042(1)	95.819(1)	95.932(1)
β (°)	125.378(1)	90.666(1)	98.674(1)	92.337(1)	98.910(1)
γ (°)	90	90	110.865(1)	107.227(1)	111.326(1)
V (Å^3)	3073.64(7)	6259.0(2)	1617.56(3)	2059.98(4)	1651.11(4)
Z	4	8	2	2	2
D_{calc} (Mg m^{-3})	1.918	2.045	2.006	2.066	1.842
F(0 0 0)	1728	3712	944	1232	896
Absorption coefficient (mm^{-1})	1.567	1.570	1.739	1.264	1.462
Crystal size (mm)	0.18 × 0.23 × 0.36	0.05 × 0.24 × 0.36	0.16 × 0.23 × 0.27	0.10 × 0.26 × 0.33	0.07 × 0.14 × 0.16
θ range (°)	2.1–35.1	1.0–31.6	1.4–35.0	1.7–30.0	1.8–35.0
Reflections collected/unique	60,267/13,566	43,813/10,450	61,271/14,123	92,293/12,007	53,063/14,419
R_{int}	0.033	0.059	0.025	0.028	0.049
Data/restraints/parameters	13,566/0/407	10,450/0/442	14,123/0/424	12,007/0/618	14,419/0/427
Goodness-of-fit (GOF) on F^2	1.26	1.02	1.03	1.03	0.99
Final R indices [$I > 2\sigma(I)$]	R_1 = 0.0455	R_1 = 0.0461	R_1 = 0.0220	R_1 = 0.0302	R_1 = 0.0405
	wR_2 = 0.0811	wR_2 = 0.1071	wR_2 = 0.0458	wR_2 = 0.0737	wR_2 = 0.0661
R indices (all data)	R_1 = 0.0608	R_1 = 0.0744	R_1 = 0.0277	R_1 = 0.0337	R_1 = 0.0651
	wR_2 = 0.0847	wR_2 = 0.1248	wR_2 = 0.0485	wR_2 = 0.0762	wR_2 = 0.0718
Largest difference peak and hole (e Å^{-3})	−1.82 and 1.64	−1.06 and 1.14	−0.54 and 0.64	−1.42 and 1.96	−0.99 and 0.86

Table 2
Bond distances (Å) in $Ru_3(CO)_{11}(L)$ complexes.

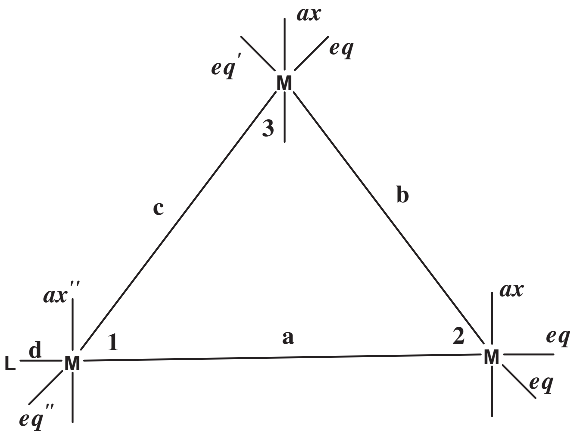

M	L	No.	M–M			M–L	M–CO					References
			a	b	c		ax[b]	eq [c]	eq'	ax''[d]	eq''	
Ru	CO		2.852(1)	2.851(1)	2.860(1)		1.942(4)	1.921(5)				[17]
Ru	CY_3 [a]		2.878(2)	2.859(2)	2.902(2)	2.425(3)	1.94	1.92	1.93(1)	1.94	1.90(1)	[20]
			2.875(2)	2.874(2)	2.920(2)	2.430(3)	1.95	1.91	1.90(1)	1.92	1.87(1)	[20]
Ru	PPh_3		2.876(3)	2.875(3)	2.907(3)	2.380(6)	1.94	1.89	1.91(3)	1.92	1.86(3)	[19]
Ru	$PPh(OMe)_2$		2.846(1)	2.858(1)	2.872(1)	2.287(1)	1.943	1.91	1.909(5)	1.933	1.888(4)	[8a]
Ru	$P(OCH_2CF_3)_3$		2.859(1)	2.846(1)	2.862(1)	2.254(1)	1.943	1.921	1.887(5)	1.931	1.911(5)	[8a]
Ru	$Ph_2P(C_6H_4Me\text{-}p)_3$	**1a**	2.8515(3)	2.8475(3)	2.8966(3)	2.3477(7)	1.941	1.923	1.930(3)	1.94	1.892(3)	[e]
Ru	$Ph_2PC_6F_5$	**1b**	2.8524(4)	2.8526(4)	2.8865(4)	2.3429(10)	1.9473	1.927	1.921(4)	1.943	1.883(4)	[e]
Ru	$P(C_6H_4Cl\text{-}p)_3$	**1c**	2.83678(14)	2.83333(15)	2.88946(14)	2.3455(3)	1.946	1.9193	1.936(14)	1.9411	1.8973(14)	[e]
Ru	$P(3,5\text{-}CF_3\text{–}C_6H_3)_3$	**1d**	2.8333(2)	2.8188(2)	2.8884(2)	2.3337(6)	1.9495	1.9324	1.926(2)	1.939	1.904(2)	[e]
Ru	$P(C_6H_4Me\text{-}p)_3$	**1e**	2.8402(3)	2.8440(2)	2.8837(2)	2.3457(6)	1.9448	1.922	1.935(2)	1.941	1.890(2)	[e]

[a] Values of two independent molecules.
[b] Average of four.
[c] Average of three.
[d] Average of two.
[e] This work.

Table 3
Hydrogen-bonding geometries (Å, °).

D–H···A	Distance (Å) D–H	Distance (Å) H···A	Distance (Å) D···A	Angle (°) D–H···A
1a				
C8–H8A···O10^{i}	0.93	2.45	3.259(4)	145
C11–H11A···O7^{ii}	0.93	2.55	3.320(5)	140
Symmetry codes: (i) $1 - x$, $2 - y$, $2 - z$ and (ii) $-x$, $-1/2 + y$, $3/2 - z$.				
1b				
None				
1c				
C3–H3A···Cg2^{i}	0.93	2.75	3.6301(15)	158
Symmetry codes: (i) $1 - x$, $-y$, $-z$; Cg2 is the centroid of benzene ring C7–C12.				
1d				
C4–H4A···O5^{i}	0.93	2.60	3.452(3)	153
Symmetry codes: (i) $1 - x$, $2 - y$, $-z$.				
1e				
C3–H3A···Cg3^{i}	0.93	2.76	3.618(3)	154
Symmetry codes: (i) $1 - x$, $1 - y$, $1 - z$; Cg3 is the centroid of benzene ring C13–C18				

Ru–CO distances range from 1.908(5) to 1.934(5) Å, [average 1.921(5) Å]. The average axial Ru–CO distances for the five complexes **1a–e** are 1.941(3), 1.946(4), 1.944(2), 1.946(2) and 1.944(2) Å respectively, which are longer than the average equatorial Ru–CO distances of 1.918(3), 1.914(5), 1.918(1), 1.925(3) and 1.918(3) Å for the complexes **1a–e** in the same order. The difference between the longest and the shortest average axial Ru–CO distances (for **1a–e**) is 0.005 Å, while the difference between the longest and the shortest average equatorial Ru–CO distances for the same complexes is 0.012 Å.

In $Ru_3(CO)_{12}$, the equatorial Ru–C–O moieties are almost linear (the average Ru–C–O angle is 178.9°) while the axial Ru–C–O moieties are slightly bent (average 172.98°) [17]. The reason for this distortion is attributed to the Van der Waals repulsion between the oxygen atoms. In the monosubstituted complexes, the equatorial CO groups (Ru–C–O bond angle) are essentially linear (average value for all the five complexes studied 176.9°, range 176.3–177.6°), while the axial CO groups are slightly bent (mean value of Ru–C–O bond angle 173.9°, range 173.8–174.1°). In the monosubstituted complexes of $Ru_3(CO)_{12}$ studied by Bruce et al., the values for the equatorial Ru–CO moieties were also linear (mean value for the complexes studied 177.5°, range 175.7–178.3°), while the angles for axial CO groups were averaging 173.3° (range 172.2–175.2°) [8a].

In $Ru_3(CO)_{12}$, the average axial OC–Ru–CO angles are 178.3° and the average equatorial OC–Ru–CO angles are 104.1°. In the monosubstituted complexes studied by us, the average axial OC–Ru–CO angles are 172.1°, 172.4°, 170.4°, 171.8° and 170.5° for the five complexes (**1a–e**); the mean value for all the complexes being 171.4°. While the average equatorial OC–Ru–CO angles are 100.7°, 98.9°, 100.5°, 101.9° and 100.9° (for **1a–e**) in the same order, the mean value being 100.6°. These observations are consistent with previously published observations of monosubstituted triuthenium cluster complexes [8a].

4. Conclusion

Several monosubstituted triruthenium cluster carbonyl complexes were synthesised with different phosphine ligands (both the PR_3 and Ph_2PR type). In all the five complexes reported, the ligands occupy equatorial positions and coordination of the ligands are only at the phosphorus atom. Due to the steric effect of the ligand, one of the metal–metal bonds is significantly longer than the other two. ^{13}C NMR spectra of the all the monosubstituted complexes showed a single broad peak for CO instead of a multiplet, exhibiting the fluxional behaviour of CO in solution. In $Ru_3(CO)_{11}P[3,5\text{-}CF_3\text{-}C_6H_3]_3$, there is disorder of the $-CF_3$ groups.

5. Supplementary data

CCDC 761605, 761606, 761607, 761608 and 761609 contain the supplementary crystallographic data for **1a–e**. These data can be obtained free of charge via http://www.ccdc.cam.ac.uk/conts/retrieving.html, or from the Cambridge Crystallographic Data Centre, 12 Union Road, Cambridge CB2 1EZ, UK; fax: (+44) 1223-336-033; or e-mail: deposit@ccdc.cam.ac.uk.

Acknowledgements

The authors would like to thank the Malaysian Government and Universiti Sains Malaysia (USM) for the Research Grant 1001/PJJAUH/811115. MAAP thanks USM for Post doctoral fellowship. HKF thanks USM for the Research University Golden Goose Grant 1001/PFIZIK/811012. CSY also thanks USM for the award of a USM Fellowship.

References

[1] L. Marko, A. Vizi-Orosz, in: B.C. Gates, L. Guczi, H. Knozinger (Eds.), Metal Clusters in Catalysis, Elsevier, Amsterdam, 1986.
[2] M.I. Bruce, J.G. Matisons, R.C. Wallis, Aust. J. Chem. 35 (1982) 935.
[3] H. Leuer, D. Schomberg, J. Organomet. Chem. 495 (1995) 53.
[4] V.M. Hansen, A.K. Biradha, R.K. Pomeroy, M.J. Zaworotko, Organometallics 17 (1998) 5267.
[5] B.F.G. Johnson, J. Lewis, D.A. Pippard, J. Chem. Soc., Dalton Trans. (1981) 407.
[6] G. Lavigne, H.D. Kaesz, J. Am. Chem. Soc. 106 (1984) 4647.
[7] M.I. Bruce, J.G. Matisons, B.K. Nicholson, J. Organomet. Chem. 247 (1983) 321.
[8] (a) M.I. Bruce, M.J. Liddell, C.A. Hughes, B.W. Skelton, A.H. White, J. Organomet. Chem. 347 (1988) 157;
(b) M.I. Bruce, M.J. Liddell, O.B. Shawkataly, I. Bytheway, B.W. Skelton, A.H. White, J. Organomet. Chem. 369 (1989) 217.
[9] A.J. Carty, S.A. Maclaughlin, N.J. Taylor, J. Organomet. Chem. 204 (1981) C27.
[10] S.T. Chacon, W.R. Cullen, M.I. Bruce, O.B. Shawkataly, F.W.B. Einstein, R.H. Jones, A.C. Willis, Can. J. Chem. 68 (1990) 2001.
[11] E. Lam, D.H. Farrar, C.S. Browning, A.J. Lough, J. Chem. Soc., Dalton Trans. (2004) 3383.
[12] (a) N. Begum, M.A. Rahman, M.R. Hassan, D.A. Tocher, E. Nordlander, G. Hogarth, S.E. Kabir, J. Organomet. Chem. 693 (2008) 1645;
(b) S.E. Kabir, E. Nordlander, Unpublished Results.
[13] O.B. Shawkataly, M.A.A. Pankhi, H.-K. Fun, C.S. Yeap, Unpublished Results.
[14] M.I. Bruce, B.K. Nicholson, M.L. Williams, Inorg. Synth. 26 (1987) 271.
[15] Bruker, APEX2, SAINT and SADABS, Bruker AXS Inc., Madison, Wisconsin, USA, 2005.
[16] G.M. Sheldrick, Acta Crystallogr. A64 (2008) 112.
[17] M.R. Churchill, F.J. Hollander, J.P. Hutchinson, Inorg. Chem. 16 (1977) 2655.
[18] K. Biradha, V.M. Hansen, W.K. Leong, R.K. Pomeroy, M.J. Zaworotko, J. Cluster Sci. 11 (2000) 285.
[19] E.J. Forbes, N. Goodhand, D.L. Jones, T.A. Hamor, J. Organomet. Chem. 182 (1979) 143.
[20] M.I. Bruce, J.G. Matisons, A.H. White, J. Chem. Soc. Dalton Trans. (1983) 2375.